Sub-nanosecond threshold-switching dynamics and set process of In_3SbTe_2 phase-change memory devices

Shivendra Kumar Pandey and Anbarasu Manivannan'

Citation: Appl. Phys. Lett. **108**, 233501 (2016); doi: 10.1063/1.4953196
View online: http://dx.doi.org/10.1063/1.4953196
View Table of Contents: http://aip.scitation.org/toc/apl/108/23
Published by the American Institute of Physics

Sub-nanosecond threshold-switching dynamics and *set* process of In_3SbTe_2 phase-change memory devices

Shivendra Kumar Pandey[1] and Anbarasu Manivannan[1,2,a)]
[1]*Discipline of Electrical Engineering, Indian Institute of Technology Indore, Indore 452020, Madhya Pradesh, India*
[2]*Materials Science and Engineering, Indian Institute of Technology Indore, Indore 452020, Madhya Pradesh, India*

(Received 19 December 2015; accepted 20 May 2016; published online 6 June 2016)

Phase-change materials show promising features for high-speed, non-volatile, random access memory, however achieving a fast electrical switching is a key challenge. We report here, the dependence of electrical switching dynamics including transient parameters such as delay time, switching time, etc., on the applied voltage and the *set* process of In_3SbTe_2 phase-change memory devices at the picosecond (ps) timescale. These devices are found to exhibit threshold-switching at a critical voltage called threshold-voltage, V_T of 1.9 ± 0.1 V, having a delay time of 25 ns. Further, the delay time decreases exponentially to a remarkably smaller value, as short as 300 ± 50 ps upon increasing the applied voltage up to $1.1V_T$. Furthermore, we demonstrate a rapid phase-change behavior from amorphous ($\sim$10 MΩ) to poly-crystalline ($\sim$10 kΩ) phase using time-resolved measurements revealing an ultrafast *set* process, which is primarily initiated by the threshold-switching process within 550 ps for an applied voltage pulse with a pulse-width of 1.5 ns and an amplitude of 2.3 V. *Published by AIP Publishing*. [http://dx.doi.org/10.1063/1.4953196]

Phase-change memory (PCM) devices have demonstrated their capabilities in the next generation high-speed, non-volatile electronic memory applications.[1–3] This is primarily owing to their unique property-portfolio of rapid and reversible switching from high-resistance amorphous (*binary* "0") to low resistance poly-crystalline (*binary* "1") state of phase-change (PC) materials by means of nanosecond electrical pulses.[4,5] Such peculiar switching characteristics are reproducible over 10^6 cycles ensuring better endurance and direct over-write capability.[6,7] Recently, GeSbTe-based PC materials have shown ultrafast crystallization/re-amorphization in sub-nanosecond timescale[8] and also a high degree of scalability with low power programming[9] that renders them ideal for phase-change logic device applications.[10,11]

Besides this, the data retention of stored bits is essentially determined by the stability of amorphous and crystalline states of PC materials. GeSbTe-based PC materials offer a relatively poor thermal stability characterized by a low crystallization temperature, T_c ($\sim$160 °C or even below).[12] In order to overcome such issues, a wide range of materials was investigated either by means of doping with other elements or modifying the device structure.[5,13] It has been recently reported that InSbTe alloys, such as In_3SbTe_2 (IST), possess an improved thermal stability compared to the GeSbTe alloys as validated by the higher crystallization temperature (above 250 °C), which favors long-term data retention.[14–16] Also, the IST material possesses a rock-salt type electronic structure similar to that of the GeSbTe materials confirming a rapid crystallization process of IST materials.[17] Furthermore, a contrast in electrical resistances of more than six orders of magnitude between the poly-crystalline and the amorphous phase of IST material promises multi-bit data storage applications such that stable intermediate resistance levels can be correlated for more than two logic states.[18] Despite their technological importance, crystallization speed of IST until now has only been achieved in the order of a few hundreds of nanoseconds.[19,20] Therefore, a systematic understanding of ultrafast switching and crystallization process of IST devices by nanosecond electrical pulses is essential.

The speed of crystallization is primarily governed by a combined effect of threshold-switching from amorphous-off (*a-off*) state to amorphous-on (*a-on*) state, followed by a crystallization (*set*) state made by Joule heating in the conducting state of PC material.[21] Therefore, these two key factors must be discerned together when high-speed crystallization of PC material is addressed. The speed of threshold-switching is essentially dictated by transient parameters such as delay time, t_d, i.e., the time elapsed prior to initiation of the switching event. Despite efforts to understand the dependence of t_d on applied voltage pulses, it has so far only been realized in the order of a few ns.[4,22] Hence, it is a challenge to realize faster crystallization made by ns electrical pulses, as it is primarily limited by the dependence on ultrafast threshold-switching transient characteristics of PCM devices. Owing to these facts, the speed of crystallization is slow compared to that of amorphization, which is the main drawback keeping us from achieving picosecond (ps) programming characteristics of the PCM devices. Therefore, a systematic understanding of time-resolved electrical pulse measurements of threshold-switching dynamics and *set* process of the PCM devices together in ps timescale is essential.

We report here, a systematic study of the dependence of transient switching parameters such as delay time, t_d, and switching time, t_s, on the applied voltage pulses of the IST cells at the ps-timescale. Our findings address a trade-off between the applied voltage pulse and the delay time revealing

a)Electronic mail: anbarasu@iiti.ac.in

a small t_d of 300 ps for 1.1 times of threshold voltage, V_T. Furthermore, our experimental results show an ultrafast *set* operation of IST devices within 550 ps.

Realizing such crystallization speeds imposes severe constraints on the measurement techniques. Hence, for reliable exploration of speed limits of PCM cells with ps electrical pulses, carefully designed high frequency contact-boards are essential.[2] Furthermore, a rapid change in dynamic resistances owing to threshold switching from *a-off* to *a-on* state causes loading and unloading of parasitic capacitances in ps, which limits the realization of the actual response of the device. In order to overcome such challenges, we used a custom-designed programmable electrical tester (PET) having a dedicated measurement line, which allows capturing the ultrafast switching dynamics of PCM cells. The PET setup consists of an Arbitrary Waveform Generator (AWG, *Agilent technologies*), a Digital Storage Oscilloscope (DSO, *Teledyne Lecroy*), a custom-made probe-station with GHz contact-boards having impedance-matching circuit (IMC) and amplifier (Amp) circuits as shown in Fig. 1(a). The IMC is designed to maintain a constant line resistance (50 Ω, same as the source and measuring end) during a rapid change of device resistances. The contact-boards were specially designed with the intent of supporting electrical pulse measurements in the ps-timescale owing to passive components that are high-frequency compatible up to 50 GHz having very small internal reactance (LC down to 1×10^{-24}). Active components are fully avoided in the direct measurement line so as to facilitate ultrafast *off-on* transitions of the PCM cells in the time-resolved data with a resolution of 50 ps. Also, to study the device response in the high-resistance amorphous phase, during which current flows typically in the range of a few nA to a few tens of μA, a high-speed amplifier circuit (Amp) is incorporated in parallel to the direct measurement line. Hence, the contact-boards provide two outputs simultaneously. One corresponds to the direct output line which provides the ultrafast *a-off* to *a-on* switching response and the second output line displays the sub-threshold current of the device.

The AWG allows voltage pulses down to a pulse-width of 1.5 ns (full width half maximum, *FWHM*), rise time, t_r, and fall time, t_f, of 1 ns having an amplitude up to 5 V and the DSO with contact-boards capable of capturing electrical characteristics at 50 ps resolution. High frequency cables used in this setup were found to have a transient response similar to that of a test pulse having t_r and t_f of 100 ps and the response time of high frequency contact-boards was found to be 250 ps. This setup, therefore, has the potential to allow overcoming the experimental challenges significantly for a reliable exploration of speed limits in the PCM devices.

In the present study, the IST phase-change thin films were RF sputter-deposited (background pressure 4×10^{-7} mbar, 20 sccm Ar flow, deposition rate of 0.0161 nm s^{-1}, operating in constant power mode of 25 W, substrate rotation of 10 rpm) on the SiO_2 substrates from a single In_3SbTe_2 stoichiometric target (*ACI Alloys Inc.*) of 99.99% purity. The amorphous nature of the as-deposited thin films was confirmed by X-ray diffraction. The composition analysis of as-deposited IST films performed by energy dispersive X-ray spectroscopic technique at over five locations reveals variations within 2 at. %. Furthermore,

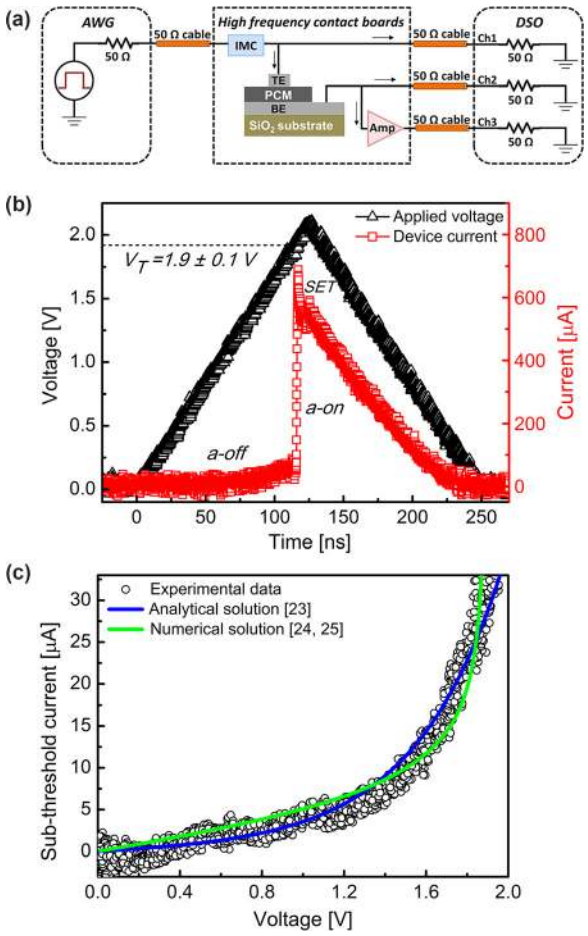

FIG. 1. (a) Schematic of custom-built programmable electrical tester consisting of an AWG, DSO, and also high-frequency contact-boards which include IMC, Amp. Also, schematic of the PCM cell structure is shown consisting of TE, IST as PCM layer and a BE in a sandwich geometry. (b) Current-voltage characteristics of the IST device for V_A (black color, triangle) having leading and trailing edge of 125 ns. Threshold-switching occurs at V_T (1.9 V), I_D (red color, square) rapidly increases from *a-off* to conducting state. During the trailing edge, I_D follows V_A indicating the formation of low-resistance poly-crystalline state. (c) Experimental data (black color, circle), analytical solutions (blue color, line), numerical solutions (green color, line) of sub-threshold conduction of IST cells. Analytical[23] and numerical solutions[24,25] are in agreement with the experimental data.

the IST cells were fabricated using IST as an active layer (thickness of 58 ± 0.3 nm), which is sandwiched between the bottom electrode (BE, thickness of 28 ± 0.2 nm) and the top electrode (TE, thickness of 28 ± 0.2 nm) of Titanium (*Ti*) on the SiO_2 substrates as shown in Fig. 1(a). Mechanical masks were used for creating specific device patterns in a cross-bar like configuration such that the BE line width is 700 μm and a short TE line width is 300 μm.

The PET setup is employed to study the dependence of transient parameters and ultrafast switching dynamics of IST cells. The electrical switching properties of several IST cells are characterized in the as-deposited amorphous (∼10 MΩ) phase. Figure 1(b) displays the time-resolved current-voltage characteristics and the switching behavior of IST cells, for an applied voltage pulse, V_A, having an amplitude of 2.0 V, leading/trailing edges of 125 ns. It can be clearly seen from Fig. 1(b) that during the leading edge of V_A, the device remains in high resistance *a-off* state below a critical voltage V_T of 1.9 ± 0.1 V. At V_T, the device current, I_D, increases

rapidly leading to a low resistance *a-on* state. Subsequent to this, the formation of a low resistance state is maintained during the trailing edge of V_A, owing to the crystallization of the conductive phase revealing a *set* process. Fig. 1(c) shows the behavior of the sub-threshold current, which indicates an ohmic conductivity at as low a voltage as 0.5 V. For higher voltages, the conductivity increases exponentially until V_T (1.9 V). The obtained experimental data on the sub-threshold conduction was found to be in agreement with the analytical solutions[23] based on the thermally assisted, trap-limited conduction (Fig. 1(c), blue line). In addition to this, numerical solutions were performed based on the literature[24,25] to validate the experimental data, which reveal the consistency of the experimental data of sub-threshold conduction (Fig. 1(c), green line). In order to further confirm the evolution of sub-threshold currents systematically, the amplitude of the V_A pulses were varied from 0.2 V to 1.7 V with a pulse pattern comprising a plateau time, t_p of 100 ns, t_r and t_f of 1 ns. It can be clearly noticed from Fig. 2(a) that for each V_A a constant sub-threshold current was observed, which increases systematically on varying V_A. The steady-state value of the sub-threshold currents for each V_A is shown in Fig. 2(b), which confirms the similar behavior of data presented in Fig. 1(b).

Furthermore, in order to obtain a precise value of the transient parameters that are associated with threshold-switching, a careful optimization of the pulse parameters of V_A is essential.[2] Typically, a steep leading edge allows the derivation of t_d precisely, the t_p controls the crystallization of the PC material, and the trailing edge indicates the status of device resistance. Therefore for the present investigation, we validate the dependency of transient parameters on V_A, by varying the pulse amplitudes from 1.8 V to 2.4 V having pulse parameters t_r, t_f of 1 ns and t_p of 100 ns.

The time-resolved ultrafast switching characteristics of numerous IST cells investigated here are in general characterized by the aforementioned specific pulse parameters. Figure 3(a) depicts the I_D measured for varying V_A from 1.8 V to 2.4 V. It can be clearly seen from Fig. 3(a) that the device remains in the *a-off* state for V_A of 1.8 V. At V_A equal to 1.9 V, the device exhibits threshold-switching with a finite t_d of 25 ns. Subsequent to this, t_d decreases rapidly for increasing V_A. Based on the literature,[26] the precise values of t_d and the t_s (switching time from *a-off* to *a-on* state, as described by change in I_D from ~30 μA to ~250 μA) are actually estimated from these measurements and are plotted in Figs. 3(b) and 3(c), respectively. Figure 3(b) displays the dependence of t_d upon V_A revealing an exponential decrease of t_d for increasing V_A. It is noteworthy to mention that a

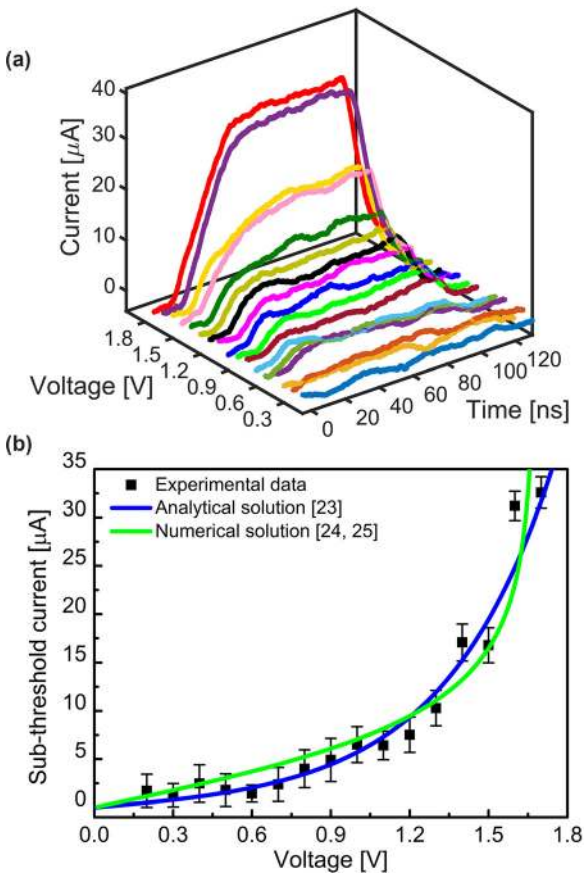

FIG. 2. (a) Evolution of sub-threshold currents for V_A (having t_r, t_f of 1 ns and t_p of 100 ns) varying from 0.2 V to 1.7 V. (b) Sub-threshold current behavior for a systematically varying V_A in conformance with Fig. 1(c).

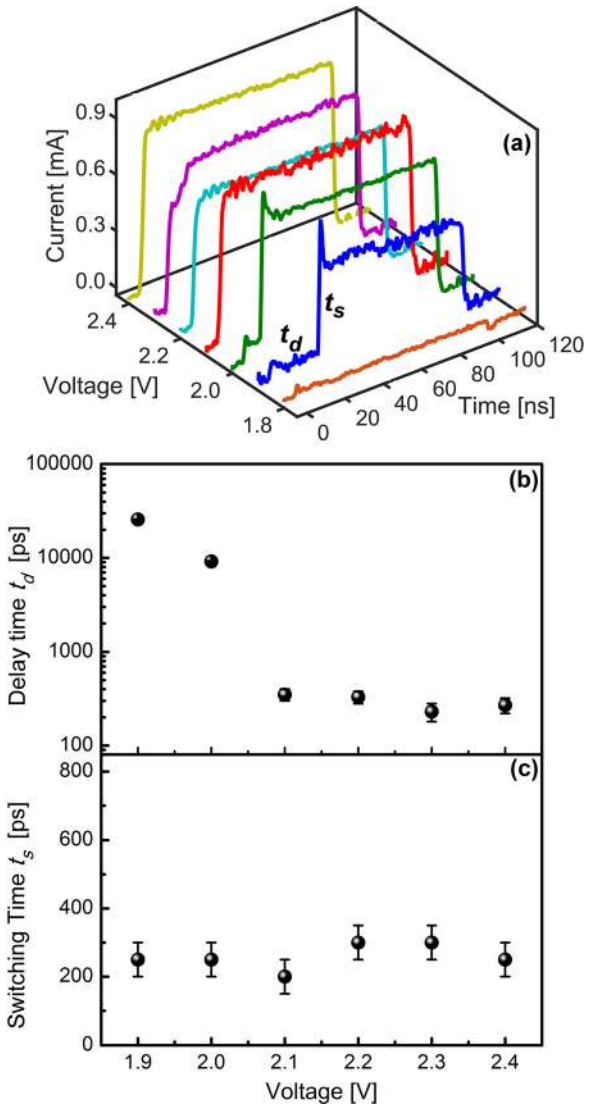

FIG. 3. (a) Time-resolved measurement of the device current I_d for voltage pulses ranging from 1.8 to 2.4 V. The overlay of I_d reveals the dependency of transient parameters such as t_d and t_s on V_A. (b) Dependence of delay time, t_d, and (c) switching time, t_s, on V_A.

strikingly small value of t_d of 300 ps is observed for a V_A of 2.1 V ($1.1V_T$), and remains as a constant value of t_d even up to a V_A of 2.4 V.

In addition to this, t_s is found to be a constant value at 250 ps for the application of various V_A, as depicted in Fig. 3(c). Therefore, it is noteworthy to mention that our experimental findings unravel a remarkably low value of t_d at 300 ps, which is about one order lower than the values reported in the literature.[4,27,28] This result confirms ultrafast switching from *a-off* to a conducting state of IST devices by the application of at least 1.1 times of V_T, demonstrating the ps-programming characteristics. This scheme of dependence of t_d would potentially be of immense help in identifying pulse parameters for ultrafast programming of the PCM devices.

In order to investigate the ultrafast *set* process of IST cells by employing the present experimental data on the dependence of the transient parameters such as t_d, we have chosen a voltage pulse with a very short pulse-width (FWHM) of 1.5 ns, amplitude of 2.3 V, t_r and t_f of 1 ns. Figure 4 displays the V_A, the response of I_D and the change of dynamic resistances corresponding to switching from the amorphous to poly-crystalline state of IST devices. It is noteworthy to mention here that I_D rapidly increases from *a-off* to a conducting state after a finite t_d of 300 ps, validating our

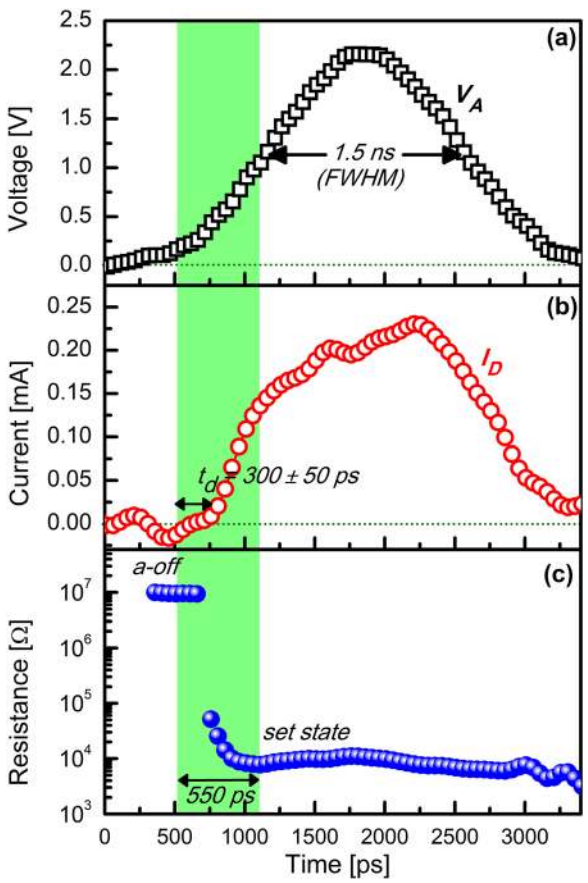

FIG. 4. Ultrafast *set* operation of IST device using (a) V_A of 2.3 V with a pulse-width of 1.5 ns (FWHM) and t_r, t_f of 1 ns. (b) I_D increases rapidly after the delay of 300 ± 50 ps indicating a rapid threshold-switching from amorphous to conducting state within 550 ps, which includes a t_d of 300 ps and a t_s of 250 ps. (c) Dynamic change of resistances from amorphous (~10 MΩ) to poly-crystalline (10 kΩ) state revealing *set* operation.

experimental findings of the dependence of t_d on V_A for even very short pulses having pulse-width of 1.5 ns (FWHM). Subsequent to this, the current flowing in the *a-on* state crystallizes the local region as depicted by the formation of a permanent low resistance state during the trailing edge of V_A, leading to the *set* operation. Evidence of this signature is the rapid transition of dynamic resistances from high resistance (~10 MΩ) amorphous state to a low resistance (~10 kΩ) state as shown in Fig. 4(c). The permanent change in resistance from amorphous to a low resistance poly-crystalline state (~10 kΩ) made by an ultrafast *set* pulse is confirmed by means of a subsequent *read* pulse (with an amplitude of 0.2 V, pulse-width of 100 ns). Therefore, this result reveals a strikingly fast *set* operation of IST devices within 1.5 ns, wherein a change in the dynamic resistance is obtained well within 550 ps, which includes a t_d of 300 ps and a t_s of 250 ps. Hence, this ultrafast threshold-switching initiated after a very short t_d of 300 ps validates the dependence of t_d as discussed above for an increased V_A of 2.3 V. Owing to this voltage-dependent transient characteristics, threshold-switching is found to occur at a lower value of V_T for an increased applied voltage of 2.3 V. This experimental observation is consistent with a theory of field induced nucleation switching in phase change materials[29–31] providing a plausible explanation that the nucleation barrier decreases exponentially with higher electrical electric fields and also the formation of needle shaped crystallites which is having lower nucleation barriers compared to spherical nuclei. Hence, for higher V_A, switching is likely to occur at a relatively lower V_T.[31] This ultrafast switching effect in the amorphous phase by means of increased V_A may therefore be looked upon as a precursor to the local ordering in the conducting region and can be compared to the concept of pre-structural ordering by means of a weak electric field induced rapid crystallization[8] using the sub-nanosecond electrical pulses owing to an increased amplitude of V_A. Therefore, the present study sheds light on the dependence of the transient parameters on V_A in ps-timescale and paves the way for achieving ultrafast programming characteristics of the PCM devices, by means of a suitable choice of pulse parameters.

In conclusion, we have demonstrated the dependence of transient switching parameters such as delay time, t_d, and switching time, t_s, on the applied voltage pulses of the IST devices at the picosecond-timescale. Our findings reveal that t_d decreases rapidly upon increasing V_A culminating in a small delay time of 300 ps for 1.1 V_T. In addition to this, the conducting state was obtained within a t_s of 250 ps from *a-off* state. Furthermore, an ultrafast *set* operation of IST devices was achieved for V_A of 2.3 V with a very short pulse-width of 1.5 ns (FWHM) revealing a rapid phase-change from a high-resistance amorphous to a low resistance poly-crystalline state that was initiated by the threshold-switching process from amorphous to a conducting state within 550 ps. These results of sub-nanosecond transient parameters and an ultrafast *set* operation of the IST devices may be of immense help towards the development of high-speed non-volatile electronic memories with gigahertz data transfer rates.

A.M. thanks the Department of Science and Technology (Grant Nos.: SB/FTP/ETA-381/2012 and SB/EMEQ-032/

2013) and Department of Atomic Energy (Grant No.: 2013/20/34/2/BRNS), Government of India for the financial support. X-ray diffraction, FE-SEM experiments were performed at the Sophisticated Instrument Centre, Indian Institute of Technology Indore.

[1]M. Wuttig and N. Yamada, Nat. Mater. **6**, 824 (2007).
[2]G. Bruns, P. Merkelbach, C. Schlockermann, M. Salinga, M. Wuttig, T. Happ, J. Philipp, and M. Kund, Appl. Phys. Lett. **95**, 043108 (2009).
[3]M. H. R. Lankhorst, B. W. S. M. Ketelaars, and R. A. M. Wolters, Nat. Mater. **4**, 347 (2005).
[4]W. Wang, L. Shi, R. Zhao, K. Lim, H. Lee, T. Chong, and Y. Wu, Appl. Phys. Lett. **93**, 043121 (2008).
[5]H. S. P. Wong, S. Raoux, S. B. Kim, J. Liang, J. P. Reifenberg, B. Rajendran, M. Asheghi, and K. E. Goodson, Proc. IEEE **98**, 2201 (2010).
[6]S. Lai and T. Lowrey, Tech. Dig.—Int. Electron Devices Meet. 36.5.1 (2001).
[7]G. W. Burr, M. J. Breitwisch, M. Franceschini, D. Garetto, K. Gopalakrishnan, B. Jackson, B. N. Kurdi, C. Lam, L. A. Lastras, A. Padilla, B. Rajendran, S. Raoux, and R. S. Shenoy, J. Vac. Sci. Technol. B **28**, 223 (2010).
[8]D. Loke, T. H. Lee, W. J. Wang, L. P. Shi, R. Zhao, Y. C. Yeo, T. C. Chong, and S. R. Elliot, Science **336**, 1566 (2012).
[9]F. Xiong, A. D. Liao, D. Estrada, and E. Pop, Science **332**, 568 (2011).
[10]D. Loke, J. M. Skelton, W. J. Wang, T. H. Lee, R. Zhao, T. C. Chong, and S. R. Elliott, PNAS **111**, 13272 (2014).
[11]M. Cassinerio, N. Ciocchini, and D. Ielmini, Adv. Mater. **25**, 5975 (2013).
[12]N. Yamada, E. Ohno, K. Nishiuchi, N. Akahira, and M. Takao, J. Appl. Phys. **69**, 2849 (1991).
[13]S. Raoux, W. Welnic, and D. Ielmini, Chem. Rev. **110**, 240 (2010).
[14]Y. Maeda, H. Andoh, I. Ikuta, and H. Minemura, J. Appl. Phys. **64**, 1715 (1988).
[15]Y. T. Kim, E. T. Kim, C. S. Kim, and J. Y. Lee, Phys. Status Solidi (RRL) **5**, 98 (2011).
[16]Y. T. Kim and S. I. Kim, Appl. Phys. Lett. **103**, 121906 (2013).
[17]V. L. Deringer, W. Zhang, P. Rausch, R. Mazzarello, R. Dronskowski, and M. Wuttig, J. Mater. Chem. C **3**, 9519 (2015).
[18]Y. I. Kim, E. T. Kim, J. Y. Lee, and Y. T. Kim, Appl. Phys. Lett. **98**, 091915 (2011).
[19]E. T. Kim, J. Y. Lee, and Y. T. Kim, Phys. Status Solidi (RRL) **3**, 103 (2009).
[20]J. K. Ahn, K. W. Park, H. J. Jung, and S. G. Yoon, Nano lett. **10**, 472 (2010).
[21]S. R. Ovshinsky, Phys. Rev. Lett. **21**, 1450 (1968).
[22]D. Adler, M. S. Shur, M. Silver, and S. R. Ovshinsky, J. Appl. Phys. **51**, 3289 (1980).
[23]D. Ielmini and Y. Zhang, J. Appl. Phys. **102**, 054517 (2007).
[24]A. Cappelli, E. Piccinini, F. Xiong, A. Behnam, R. Brunetti, M. Rudan, E. Pop, and C. Jacoboni, Appl. Phys. Lett. **103**, 083503 (2013).
[25]F. Buscemi, E. Piccinini, A. Cappelli, R. Brunetti, M. Rudan, and C. Jacoboni, Appl. Phys. Lett. **104**, 022101 (2014).
[26]S. Lavizzari, D. Ielmini, and A. L. Lacaita, IEEE Trans. Electron Devices **57**, 3257 (2010).
[27]M. Anbarasu, M. Wimmer, G. Bruns, M. Salinga, and M. Wuttig, Appl. Phys. Lett. **100**, 143505 (2012).
[28]M. Wimmer and M. Salinga, New J. Phys. **16**, 113044 (2014).
[29]V. G. Karpov, Y. A. Kryukov, S. D. Savransky, and I. V. Karpov, Appl. Phys. Lett. **90**, 123504 (2007).
[30]I. V. Karpov, M. Mitra, D. Kau, G. Spadini, Y. A. Kryukov, and V. G. Karpov, Appl. Phys. Lett. **92**, 173501 (2008).
[31]V. G. Karpov, Y. A. Kryukov, M. Mitra, and I. V. Karpov, J. Appl. Phys. **104**, 054507 (2008).